

A TEMPO-substituted polyacrylamide as a new cathode material: an organic rechargeable device composed of polymer electrodes and aqueous electrolyte

Kenichiroh Koshika, Natsuru Chikushi, Naoki Sano, Kenichi Oyaizu and Hiroyuki Nishide *

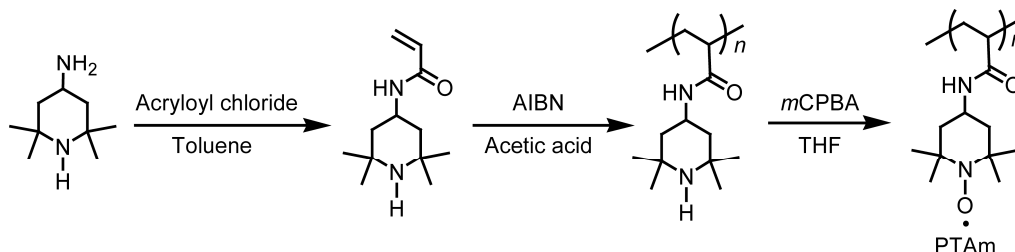
Department of Applied Chemistry, Waseda University, Tokyo 169-8555, Japan

Electronic Supporting Information

Table of Contents

1. Synthesis of Poly(2,2,6,6-tetramethylpiperidinyloxy-4-yl acrylamide) (PTAm)
2. AFM image of PTAm electrode
3. Charging-discharging performance of PTAm electrode (half-cell)

1. Synthesis of Poly(2,2,6,6-tetramethylpiperidinyloxy-4-yl acrylamide) (PTAm)



Scheme S1 Synthesis of the TEMPO-substituted polyacrylamide.

1.1 Preparation of 2,2,6,6-tetramethylpiperidine-4-yl acrylamide

Acryl chloride (1.3 ml) was dropwise added to an ice-cold solution of 4-amino-2,2,6,6-tetramethylpiperidine (2.8 ml) in anhydrous toluene (60 ml) and triethylamine (0.9 ml) under an argon atmosphere with magnetic stirring. The mixture was vigorously stirred for 1 h at 5°C and then for 1 h at room temperature. At the end of the reaction, the precipitate was collected by filtration, extracted with dichloromethane and washed with aqueous K₂CO₃. The solvent was removed in vacuo, and the residue was purified using a silica gel column with ethyl acetate. An appropriate fraction was collected and crystallized from an ethanol/hexane mixed solution. The acrylamide monomer was isolated as white crystals (1.1 g).

The elemental analysis: C, 68.7; H, 10.7; and N, 13.2; Calcd. for $C_{11}H_{20}NO_2$: requires C, 68.5; H, 10.5; and N, 13.3. δH (500 MHz; $CDCl_3$; Me_4Si) 6.28 (1H, d, $J = 1.5$ Hz, vinyl CH_2), 6.06 (1H, q, $J = 10.4$ Hz, vinyl CH), 5.63 (1H, dd, $J = 1.5$ Hz, vinyl CH_2), 5.29 (1H, s, amide NH), 4.35 (1H, d, $J = 12.2$ Hz, piperidine CH), 1.94 (2H, dd, $J = 4.0$ Hz, piperidine CH_2), 1.27 (6 H, s, $2 \times CH_3$), 1.13 (6 H, s, $2 \times CH_3$) 0.94 (2H, t, $J = 12.2$ Hz, piperidine CH_2); δC (500 MHz; $CDCl_3$; Me_4Si) 28.5, 34.9, 42.7, 45.2, 51.1, 126.4, 131.0, 164.8. Mass: m/z , 211.2 (found), 210.3 (calcd).

1.2 Radical polymerization of the acrylamide monomer

2,2,6,6-Tetramethylpiperidine-4-yl acrylamide (320 mg) was dissolved in Acetic acid (1.0 ml). 2,2'-Azobisisobutyronitrile (AIBN) (1.6 mg) was added to the solution. The glass ampoule containing the solution was sealed. The solution was then heated for 4 h at 70°C. The resulting solution was evaporated, and dissolved in a small amount of chloroform. The solution was dropwise added to chloroform/diethylether (1/1 v/v 100 ml). The precipitate was collected by filtration, and dried under reduced pressure for 12 h. Poly(2,2,6,6-tetramethylpiperidine-4-yl acrylamide) was obtained as a white powder (27 mg).

Elemental analysis of poly(2,2,6,6-tetramethylpiperidine-4-yl acrylamide): C, 68.1; H, 10.9; and N, 13.2; Calcd. for $C_{11}H_{20}NO_2$: requires C, 68.5; H, 10.5 and N, 13.3. The precursor polymer was characterized by NMR spectroscopy. δH (500 MHz; $CDCl_3$; Me_4Si) 6.28 (1 H, br s, amide NH), 4.20 (1 H, m, piperidine CH), 2.21 (1 H, br s, alkyl CH_2), 1.85 (2 H, br s, piperidine CH_2), 1.66 (1 H, br s, alkyl CH_2), 1.25 (6 H, s, $2 \times CH_3$), 1.12 (6 H, s, $2 \times CH_3$), 1.00 (2 H, br s, piperidine CH_2), 0.65 (1 H, br s, alkyl CH_2); δC (500 MHz; $CDCl_3$; Me_4Si) 28.7, 29.0, 35.1, 42.3, 42.7, 45.2, 51.0, 174.4.

1.3 Oxidation of poly(2,2,6,6-tetramethylpiperidine-4-yl acrylamide)

Poly(2,2,6,6-tetramethylpiperidine-4-yl acrylamide) (150 mg) was added to ice-cold solution of *m*-chloroperbenzoic acid (620 mg) in THF (5 ml), and stirred for 3 h at room temperature. The polymer was dissolved in THF with oxidation. The solution was dropwise added to diethylether/hexane (1/1 v/v 200 ml). The precipitate was collected by filtration, and dried under reduced pressure for 12 h. Poly(2,2,6,6-tetramethylpiperidinyloxy-4-yl acrylamide) was obtained as an orange powder (140 mg). The molecular weight of the polymer was $M_w=1,100,000$ with a dispersity of $M_w/M_n=4.9$.

1.4 Characterization of the radical polymer

The TEMPO radical moiety of the PTAm was characterized by ESR spectroscopy and SQUID magnetic measurements. The PTAm powder gave a single broad ESR at $g = 2.0067$ (**Fig. S1**) corresponding to that of TEMPO (2.0056). The broadening of the ESR spectrum is explained by intrachain dipole-dipole interaction due to the close distance among the polymer-bound radical sites.

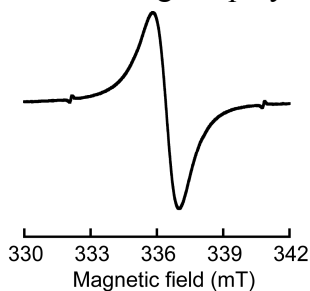


Fig. S1 ESR spectrum of the powder sample of PTAm.

The unpaired electron density in the PTAm was determined from the $1/\chi_{\text{mol}}$ versus T plots (**Fig. S2**), based on the Curie-Weiss rule according to $1/\chi_{\text{para}} = T/C - \theta/C$ where C is a Curie constant defined as $N_e g^2 \mu_B^2 S(S+1)/(3k_B)$. The slope of the $1/\chi_{\text{mol}}$ versus T plots corresponded to $1/C$ and gave an unpaired electron density of $N_e = 1.95 \times 10^{21}$ spin/g for the PTAm. The linear relation was ascribed to a typical paramagnetic behavior of the unpaired electrons of the PTAm, and its slope gave the unpaired electron or radical concentration of the PTAm sample, in the example of Fig. S2, of 0.96 per monomer unit of the PTAm. A maximum effective charging-discharging capacity per weight of 114 mAh g^{-1} was calculated using the formula-weight-based charging-discharging capacity of $119 \text{ mAh g}^{-1} \times 0.96$. The unpaired electron concentration was almost maintained over three months under ambient conditions.

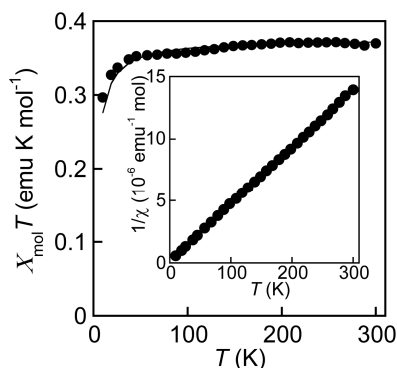


Fig. S2 Plots of $1/\chi$ (15 mg) vs. temperature (Curie-Weiss plots) for the powder sample of PTAm. Inset: ESR spectrum of the powder sample of PTAm.

2. AFM image of PTAm electrode

A microscopic analysis revealed that the polymer film surface was uniformly dense without any defects.

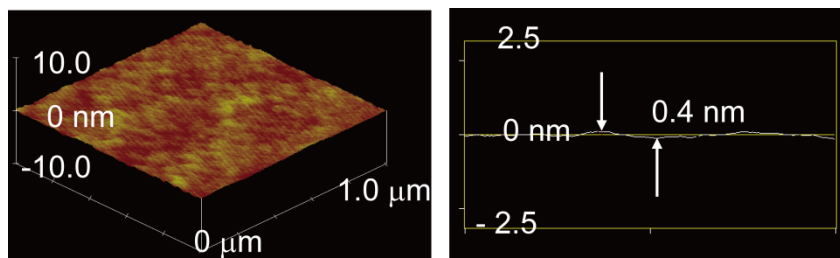


Fig. S3 AFM image of PTAm film with smooth surface (a roughness of ± 0.2 nm) before the electrochemical measurements.

3. Charging-discharging performance of PTAm electrode (half-cell)

3.1 Charging-discharging performance

The charging-discharging curves of the half cell exhibited a plateau voltage at $0.66 \square 0.71$ V vs. Ag/AgCl (**Fig. S4**), which agreed with the redox potential of the PTAm film (0.68 V) shown in the Inset of Fig. 2 (a). The charging-discharging capacities almost coincided with each other at ca. 114 mAh g^{-1} and agreed with the calculated capacity obtained in Fig. 2 (a) ($4.1 \text{ mC cm}^{-2} \times 100 \text{ nm}$ thickness).

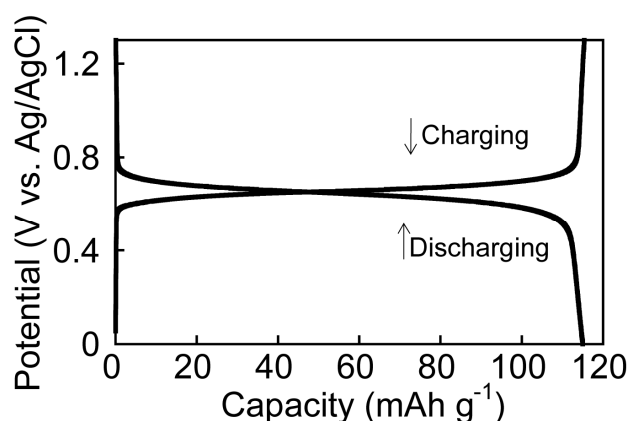


Fig. S4 Charging-discharging curve of the PTAm film at charging-discharging rate of 60 C ($68 \mu\text{A cm}^{-2}$).

3.2 Charging-discharging cycle performance

The cycle performance of the charging-discharging at the cut-off voltages of 0.4–0.9 V and C-rate of 60 C is shown in **Fig. S5**. The coulombic efficiency, i.e., discharging capacity vs. charging capacity, is maintained at almost 100% even after 10,000 charging-discharging cycles, indicating that the charged species, the oxoammonium form of the PTAm, stoichiometrically contributed to the following discharging process. The discharging capacity was maintained to ca. 85% of the initial value after 10,000 cycles, suggesting no partial elution out of the PTAm polymer into the electrolyte.

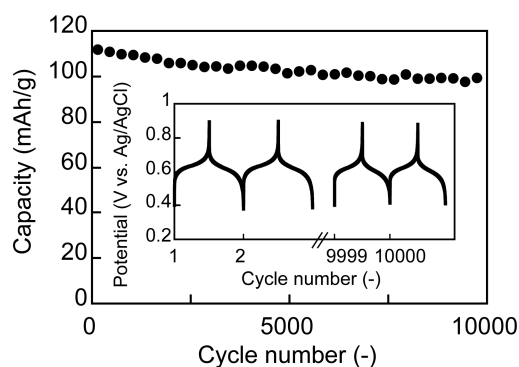


Fig. S5 Discharging capacity for the half-cell composed of the PTAm film vs. the charging-discharging cycle number at the charging-discharging rate of 60 C. Inset: Charging-discharging curves of the PTAm film.